

New 3D in Silico Model of Hair and Skin Heating During Laser Hair Removal

Gregorio Viera Mármol^{1*}, Jorge Villena¹

¹Cocoon Medical S.L.U., Barcelona, Spain

*Correspondence: gregorioviera@cocoonmedical.com; Tel.: +3493458566

Abstract — The efficacy and safety of conventional laser hair removal technology is fundamentally based on clinical case studies. However, the internal temperature of hair during treatment and thus the efficacy of the laser pulse cannot be measured or evaluated. Also the level of heat that reaches the surrounding skin tissue is just estimated in order to prevent burning. In this sense, any method that enables the measurement of the temperature that reaches the hair and skin during a laser pulse is a potential tool to improve laser hair removal technique and to increase the safety of laser technology.

Here we develop new numerical multiphysics simulation software to simulate the hair removal process. We create 3D models of dermal tissue that include the epidermis, dermis and hair follicle structure. Subsequently, laser pulses of 755 nm, 810 nm and 1064 nm with different power and pulse characteristics have been simulated. Through a process of numerical calculation, we simulated the heating of skin and hair follicles with various characteristics and determined the temperature and thermal damage in order to anticipate the efficacy and safety of laser hair removal. We show that the best results are obtained with shorter pulse durations and, therefore, with the highest laser power. Moreover, we demonstrate that longer wavelengths (1064 nm) provide better efficacy and safety for dark skin. The model developed in this study can be used to gain a better understanding of the laser hair removal process, to conduct clinical studies, develop better and safer devices, and to assist clinicians in the selection of parameters for achieving optimal and safe results during hair removal procedures.

Keywords — Laser hair removal, in silico model, simulations, computer modeling.

I. INTRODUCTION

Even though laser hair removal is a commonly used technique worldwide, the measurement of the temperature that reaches the hair and surrounding skin during laser impulse is practically impossible to determine. This information is not only necessary to assure the efficacy of the treatment, most importantly, it is necessary to guarantee the safety of the patient. Laser treatment is accomplished via a pulsed energy source where parameters such as fluence, pulse duration and frequency can be modulated, while the area of interaction and wavelength are fixed by the device. In order to protect the surrounding skin, a cold sapphire crystal with a size and shape specifically designed for skin refrigeration purposes is commonly employed during irradiation. Sapphire is used for the tip because it has high thermal conductivity and hardness.

To produce thermal damage of undesirable hair, the parameters of the laser should be carefully configured, primarily based on the content of melanin within the hair and surrounding skin. Ideally, each patient should have a personalized treatment set-up, based on their individual characteristics. Several clinical studies describe the efficacy of laser treatment in terms of irreversible hair removal and the evaluation of pain [1–3], however the temperature models are scarce. In fact, there are not reliable methodologies to obtain the internal temperature of the hair, and as a consequence, a relatively long period of time (several weeks or months) is required to effectively validate the results of laser hair removal. In this sense, any method that enables the evaluation of hair temperature and its corresponding thermal damage would be a potential tool to improve laser hair removal technique and develop lasers that are specifically optimized for this application.

In general, the sector often opts for Solid State Lasers (SSL) (e.g. Alexandrite SSL) since this type of laser can reach a very high power (15,000 W), which allows very short duration laser energy pulses (up to 3 ms) to be worked with. The higher the laser power, the shorter the laser pulse that can be used and the more effective the process of heating the hair structure is. Additionally, stem cells responsible for hair regrowth that are located in the vicinity of the bulge [4–5] are also heated as a result of laser irradiation, which can cause their destruction and produce permanent hair removal. However, even though Alexandrite lasers dominate the world market for laser hair removal systems, this equipment has certain limitations and/or disadvantages. It offers just less than 10% efficiency with respect to the electric power used and a special electrical installation is required. This limits the operation frequency to 1–2 Hz and makes the procedure relatively slow. Besides, it requires consumables as well as very expensive and frequent maintenance and has an elevated fabrication price.

An alternative is the diode laser based systems, which are much more efficient (close to 50% in terms of electrical energy) and thus can be used with common electrical installations. Diode lasers operate using frequencies higher than 10 Hz and therefore allow faster treatments without consumables or the need for continuous maintenance. They also have a much lower market price compared to SSL. The main disadvantage of diode lasers is the relatively low laser power. Therefore, the laser pulse used has to be much longer and produces less effective heat transmission to the hair and surrounding cells due to the initiation of cooling processes. Despite this, diode lasers offer substantial technological advantages that justify their presence in the market.

TABLE 1: Factors that can be modulated in the new 3D in silico model

I. Skin	Epidermis thickness	Epidermis skin type I to VI	Scattering coefficient	Water content	Blood content				
II. Hair	Shaft diameter	Bulb diameter	Hair depth	Bulb blood content	Color				
III. Laser beam /sapphire tip	Pulse energy	Pulse duration	Wavelength	Frequency	Overlapping	Beam homogeneity	Beam size	Sapphire cooling temperature	Hair-removal gel thickness

Importantly, the laser power and duration of the pulse are not the only factors responsible for efficient hair removal. Multiple clinical studies have determined the optimal conditions for hair removal depending on the type of hair and skin. The range of fluence, frequency and wavelength of laser power has been specified for each patient category [2–3].

Here, we use new multiphysics simulation software to create a three-dimensional (3D) model of the dermal tissue—formed by the epidermis, dermis and hair structure—which is subject to pulsed laser treatment. As a scaffold, we used COMSOL Multiphysics® simulation software, which allows the use of several physical variables and assembling at the same time.

Laser pulses of 755 nm, 810 nm and 1064 nm with different parameters and various hair and skin types have been simulated. We have determined the heating and thermal damage of the skin and hair under laser irradiation. The results can be used to anticipate the safety and efficacy of different laser settings.

II. MATERIALS AND METHODS

2.1. 3D simulation of hair and skin heating using COMSOL Multiphysics® software

We have developed a realistic 3D model for hair and skin heating during laser hair removal with real dimensions of the: i) sapphire (upper layer), ii) epidermis, iii) dermis and iv) hair (Fig. 1). In order to simulate the cooling of the skin, a sapphire crystal with a particular size and shape, specifically designed for skin refrigeration purposes, has been considered in the model. Our 3D model allows the modulation of a wide spectrum of possible variations in terms of skin, hair and laser settings, which influence laser hair removal (Table 1).

The existence of a hair-removal gel layer with a thickness of 0.3 mm between the sapphire and skin has also been considered. The epidermis layer has been set at 60 μm [6]. Hair has been divided into three zones: upper shaft, lower shaft and bulb (Fig. 1A and 1B).

Regarding the hair model, different dimensions were considered (Table 2). In addition, different hair densities were used during simulation, however, after observing that the results did not change with the density, this variable was omitted. Two types of hair have been considered: untreated or original hair with fine and thick dimensions, and the so-called “residual” that is the treated hair.

In order to precisely simulate hair and skin heating during laser hair removal, COMSOL Multiphysics® software was used to assemble a Helmholtz equation describing tissue light diffusion, a heat transfer equation describing heating, and an Arrhenius equation describing thermal damage (described in detail below).

TABLE 2: Hair parameters used in the simulation. The residual term is used for thinned hair after hair removal treatments [7, 8, 9].

Type of hair	Depth (mm)	Bulb radius (mm)	Shaft radius (mm)
Untreated fine	2,5	0,094	0,03
Untreated thick	3,5	0,141	0,04
Residual fine	2,5	0,047	0,02
Residual thick	3,5	0,047	0,02

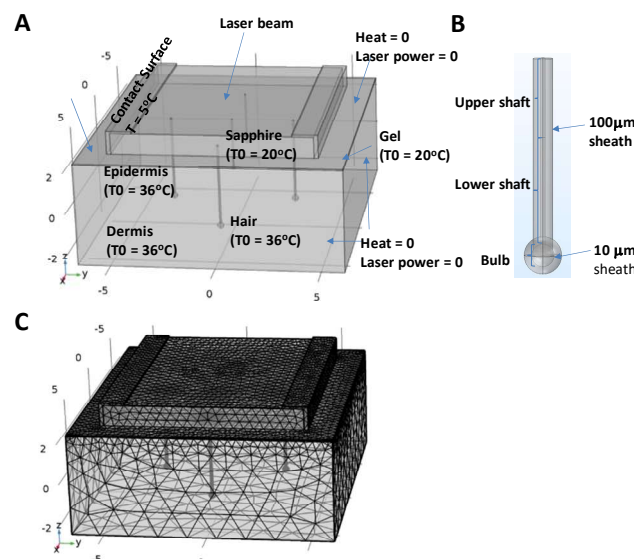


Figure 1: 3D model of hair and skin heating. The 3D model includes a layer of epidermis (60 μm, T0 = 36°C), dermis (T0 = 36°C) and hair (T0 = 36 °C). The sapphire crystal (T0 = 20°C) and a gel layer between the sapphire and skin (0.3 mm, T0 = 20°C) have also been included (A). The hair model has been divided into three zones: upper shaft, lower shaft and bulb. Two different sheath areas (10 μm and 100 μm) have been considered (B). The geometric model used in the numerical simulation has been separated into a fine mesh in which the numerical equations for light diffusion, heat transfer and thermal damage have been solved simultaneously (C).

A finite element calculation method was employed to find the temperature matrix of the 3D system. The geometric model used in the numerical simulation was separated into a fine mesh in which the numerical equations for light diffusion, heat transfer and thermal damage have been solved simultaneously (Fig. 1C).

The resultant temperatures and values for thermal damage that were used to compare the results of the simulations represent the average values for the epidermis, hair shaft and hair bulb.

2.2. Helmholtz light diffusion differential equation

The following differential equation describes the diffusion of light within a certain environment, in our case the skin:

$$\frac{\partial \Phi}{\partial t} - D \nabla^2 \Phi + c \mu_a \Phi = 0$$

where Φ is the power intensity of the laser light pulse, D is the optical diffusion coefficient for each tissue (epidermis, dermis and hair), c is the speed of light and μ_a is the absorption coefficient for each tissue.

The optical diffusion coefficient can be defined as follows:

$$D = \frac{c}{3(\mu_a + ((1-g) \cdot \mu_s))}$$

where μ_s is the scattering coefficient and g is the anisotropy coefficient of light for each tissue.

The only surface with power intensity was the surface of the epidermis through the sapphire windows (Fig 1A). All the other surfaces were considered as isolated in the simulation.

Regarding the initial conditions, the laser pulse started at a time of zero. The power intensity followed a square top-hat spatial pattern (Fig 2). This is the main distribution profile of the laser diodes, in which the energy is evenly distributed over its entire area.

$$\mu_a = (f_{mel} \cdot (f_{eu} \cdot \mu_{eu} + (1 - f_{eu}) \cdot \mu_{pheo})) + (1 - f_{mel}) \cdot \mu_{skin}^{baseline}$$

Regarding the studied tissues (epidermis, dermis and hair), scattering must be taken into account in the dermis. In the hair and epidermis the scattering can be neglected due to small dimensions which do not allow the light to scatter. Therefore, the dermis is the only scattering medium in our model and its scattering coefficient was considered [16, 17] accordingly:

$$\mu_s = X \cdot \frac{577}{\lambda}$$

In our model, $X = 25,000$, as described in previous work [17].

Melanin is the main chromophore of the skin and hair that absorbs the laser energy. It contains a mixture of proteins called eumelanin and pheomelanin. For the epidermis, skin types (I–VI) are defined according to the Fitzpatrick scale. The absorption coefficients for the various skin types were calculated from the absorption spectra of eumelanin and pheomelanin according to Donner & Jensen [10].

$$\mu_a = (f_{mel} \cdot (f_{eu} \cdot \mu_{eu} + (1 - f_{eu}) \cdot \mu_{pheo})) + (1 - f_{mel}) \cdot \mu_{skin}^{baseline}$$

where f_{mel} and f_{eu} are the melanin and eumelanin factors of the different skin types, μ_{eu} and μ_{pheo} are the absorption coefficients of eumelanin and pheomelanin, and $\mu_{skin}^{baseline}$ is the base absorption coefficient of the skin, where the absorption coefficient of eumelanin has a much stronger wavelength dependence than the coefficient of pheomelanin and the base absorption coefficient of the skin [10]. The eumelanin factor has been considered constant for all skin types ($f_{eu} = 0.7$) while the melanin factor was dependent on the skin type as defined according to Donner & Jensen [10] and Jacques [11].

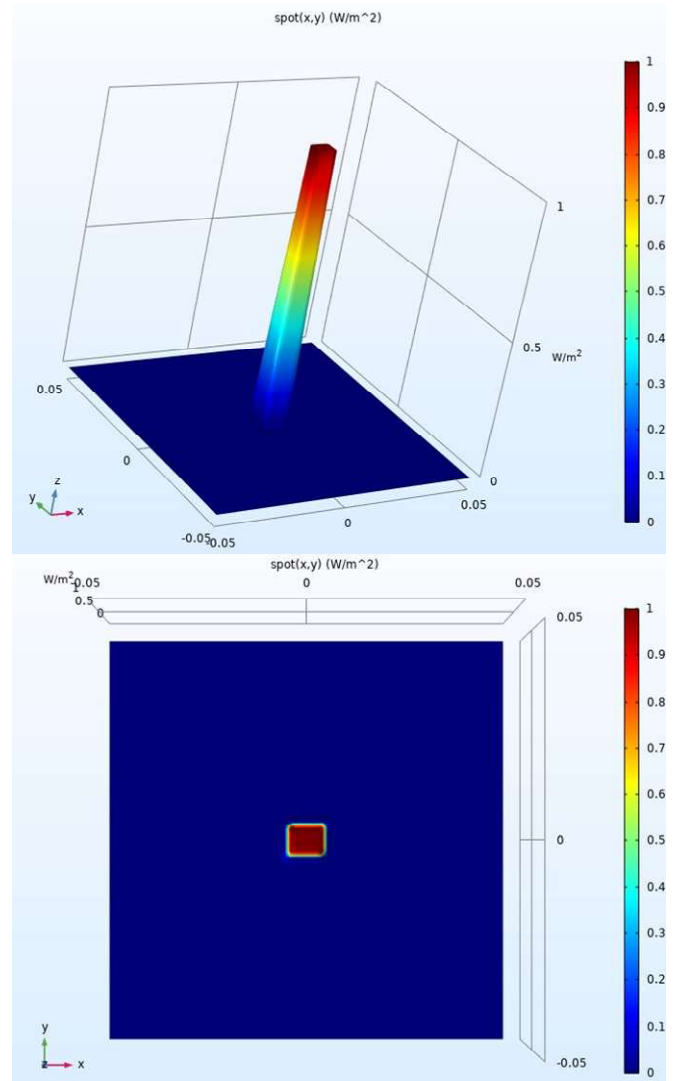


Figure 2: Laser beam intensity in 3D (up) and laser beam spot (down)

We also considered the presence of water and blood in the dermis. The water absorption coefficient is dependent on wavelength according to Kou, Labrie, & Chylek, (1993) [13]. It is almost negligible for the 760 nm and 810 nm wavelengths ($\sim 2 \text{ m}^{-1}$) and the variation produced if water absorption is not considered in the simulation is less than 3%. However, for a 1060 nm laser, the water absorption is not negligible ($\sim 20 \text{ m}^{-1}$) and produced differences of up to 10% in the results of the simulation. We considered a fractional amount of water in the dermis of 70%.

Blood absorption was considered to be uniformly distributed in the dermis according to the equation (18) [10].

Therefore, the total absorption coefficient of the dermis regarding blood and water is as follows:

$$\mu_a(\lambda) = C_h \times [\gamma \times \mu_{blood}^{oxy}(\lambda) + (1 - \gamma) \times \mu_{blood}^{deoxy}(\lambda) - \mu_{skin}^{baseline}] + C_{H_2O} \times \mu_{H_2O}$$

where C_h is the fractional amount of hemoglobin in the dermis (usually from 0.1%–10%), μ_{blood}^{oxy} is the absorption of oxy-hemoglobin, μ_{blood}^{deoxy} is the

absorption of deoxy-hemoglobin, $\mu_{skin}^{baseline}$ is the base absorption coefficient of the skin and γ is the blood oxygenation ratio between deoxy-hemoglobin and oxy-hemoglobin. In our model $\gamma = 0.75$. The blood absorption coefficient was obtained from the absorption coefficients of the two types of hemoglobin [14, 15]. C_{H_2O} is the fractional amount of water in the dermis, in our case it is considered to be 70%.

Finally, the absorption coefficient of the hair was also dependent on the amount of melanin. The simulation was made for light (blond), dark brown and black hair. The absorption coefficient of each kind of hair was chosen according to T. van Kampen [12].

$$\begin{aligned} \text{Blond:} \quad \mu_a &= 5222,21 \cdot e^{(-5,56 \cdot 10^{-4} \lambda)} \\ \text{Dark Brown:} \quad \mu_a &= 25150,83 \cdot e^{(-1,37 \cdot 10^{-3} \lambda)} \\ \text{Black:} \quad \mu_a &= 38421,55 \cdot e^{(-1,60 \cdot 10^{-3} \lambda)} \end{aligned}$$

where λ is the wavelength in nm.

2.3. Heat transfer equation for biomaterials

The laser power that is absorbed by the tissues is transformed into heat and produces an increase in temperature according to the following equation:

$$\begin{aligned} \rho C_p \frac{\partial T}{\partial t} + \nabla \cdot q &= Q + Q_{bio} \\ q &= -k \nabla T \end{aligned}$$

For each material used in the simulation, ρ is the density, C_p is the specific heat capacity at constant pressure, k is the thermal conductivity, T is the absolute temperature, q is the heat flux by thermal conduction, Q_{bio} is the biological heat source and Q is the heat generated by laser absorption. Biological heat (Q_{bio}) represents a combination of blood perfusion (or blood flow) and metabolic heat. We considered biological heat as negligible, since the laser pulse duration is in the range of milliseconds which is not long enough to necessitate considering any change in either blood perfusion or metabolic heat [25].

Table 3 shows the parameters for the materials used in the simulations: sapphire, epidermis, dermis and hair.

TABLE 3: Summary of tissue parameters: thermal conductivity (k), specific heat (C_p), and density (ρ). (Epidermis [19, 20], Dermis [18, 20], Hair [18, 19], Sapphire [21, 22])

Tissue	k (W/m·K)	C_p (J/kg·K)	Density (kg/m ³)
Epidermis	0.21	3600	1200
Dermis	0.53	3800	1200
Hair	0.24	3500	1300
Sapphire	40	750	3980

The temperature T was calculated with respect to the initial temperature T_0 :

$$T = \Delta T + T_0$$

where ΔT is derived from the solution of the heat transfer equation.

For the biological tissues (hair, epidermis and dermis) $T_0 = 36^\circ\text{C}$ and for non-biological materials (sapphire) $T_0 = 20^\circ\text{C}$. Regarding heat flux, for all surfaces except the one below the laser spot, the heat flux was 0.

2.4. Arrhenius equation of thermal damage

Thermal tissue damage was described by the Arrhenius equation:

$$\Omega = \int_0^t A e^{-E_a/RT}$$

where Ω is the rate of tissue damage, A is the frequency factor, E_a is the activation energy, R is the constant of the ideal gases and T is the temperature. This equation calculates the damage accumulated in the tissue over time. In our 3D model, $E_a=6.27 \times 10^8$ J/mol and $A=3.1 \times 10^{98}$ s⁻¹, which are the most commonly used constant values for the working temperatures [23].

In addition, we calculated θ_d which represents the fraction of necrotized tissue according to:

$$\theta_d = 1 - e^{-\Omega}$$

where the θ_d parameter provides a representation of the hair removal efficacy.

In order to calculate the thermal damage of the cells in close vicinity to the hair, two sheath sizes were drawn up wrapping the hair with the properties of the dermis: one at 10 μm from the surface of the bulb (the minimum distance at which the simulation program can solve the equations) to calculate the temperature and the thermal damage of the cells located on the bulb that are responsible for hair growth, and the other at 100 μm from the surface of the shaft to calculate the thermal damage of the stem cells located in the bulge that are responsible for its re-growth [5].

The average values of the fraction of the necrotic tissue for the different areas of hair and sheaths were obtained from the simulation.

Moving forward, multiple tests were carried out considering all the parameters subject to the 3D model (table 1). We determined the temperature of skin, hair and cells and the resultant thermal damage depending on the laser parameters (fluence, pulse duration, frequency, wavelength and spot size) for each skin type and set of hair characteristics.

III. RESULTS

3.1. Evaluation of the safety of laser hair removal using the in silico 3D mathematical model.

In order to guarantee the safety of the patient during laser hair removal, the temperature of the epidermis should not exceed 43°C during the procedure. We have used our 3D model to calculate the epidermis temperature that would be reached during laser hair removal using various laser settings and skin types.

First, we investigated the temperature that the epidermis would reach depending on the fluence used and we observed that the temperature increased linearly with the fluence. Figure 3A shows an example with a laser pulse of 810 nm, 30 ms and 3 Hz on skin type III, with a fluence of 30 J/cm² and 55 J/cm².

After a laser pulse of 30 J/cm² the temperature of the epidermis was 44.3°C, while a laser pulse of 55 J/cm² heated the epidermis to 63.5°C (Fig. 3A).

In addition, we investigated the temperature that the epidermis reaches under constant fluence but with variable skin types. Simulations showed that temperature increases with skin type. Figure 3B shows an example with a laser pulse of 810 nm, 20 J/cm², 10 ms and 3 Hz which heated the epidermis to 22°C with skin type I, while 43°C was obtained with skin type III (Fig. 3B). When the simulation was performed at 1 Hz, the results were slightly different: 19°C with skin type I and 40°C with skin type III (example not shown).

When we investigated the effect of wavelength, we observed that the temperature of the epidermis decreases with increasing wavelength. When a laser pulse of 755 nm, 20 J/cm², 10 ms and 3 Hz was used, the epidermis reached 56.5°C, while for the same laser pulse at 1060 nm, the epidermis reached 33.1°C (Fig. 3C).

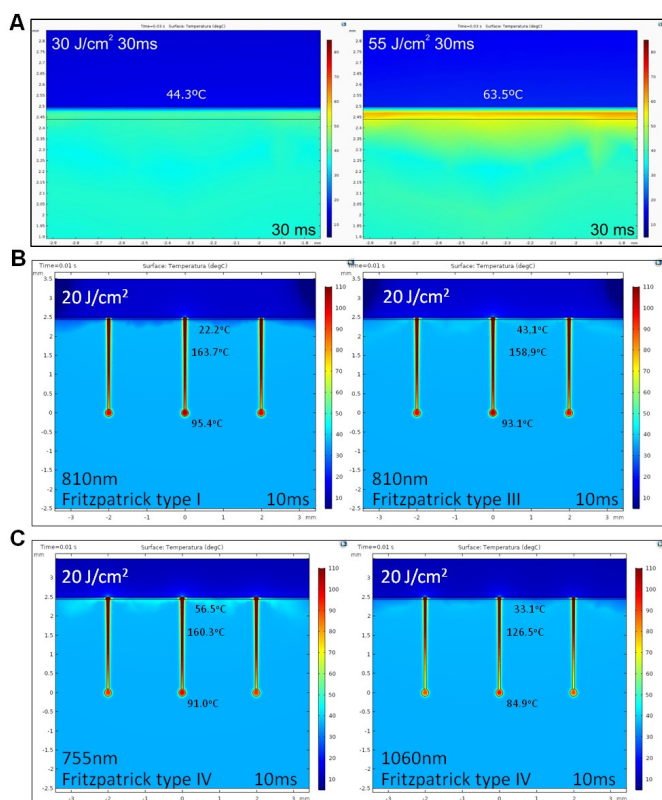


Figure 3: Example of hair and skin heating simulation results. Laser pulses with an energy level of 30 J/cm² heat the epidermis to 44.3°C, while laser pulses with an energy level of 55 J/cm² heat the epidermis to 63.5°C (A). Laser pulses of 810 nm, 20 J/cm², 10 ms and 3 Hz heat the epidermis to 22°C with skin type I, while skin type III heats to 43°C (B). For skin type IV, with laser pulses of 755 nm the epidermis reaches 56.5°C, while laser pulses of 1060 nm heat the epidermis to 33.1°C, according to in silico simulation (C).

Figure 4 summarizes the results of multiple simulations where we outline the maximum simulated fluence for 755 nm, 810 nm and 1060 nm diode lasers of 4,000 W operating at 3 Hz on all skin types, which should not exceed an epidermal temperature of 43°C during use to guarantee patient safety

(Fig. 4). For 755 nm and 810 nm, skin type I and II can operate safely up to 40 J/cm². Notably, 1060 nm laser diodes can operate safely at 40 J/cm² up to skin type IV. The limits for higher numbered skin types are as follows: skin type III, 14 J/cm² at 755 nm and 19 J/cm² at 810 nm; skin type IV, 10 J/cm² at 755 nm and 14 J/cm² at 810 nm; skin type V, 4 J/cm² at 755 nm, 5 J/cm² at 810 nm and 14 J/cm² at 1060 nm; and skin type VI, 2 J/cm² at 755 nm, 3 J/cm² at 810 nm and 6 J/cm² at 1060 nm.

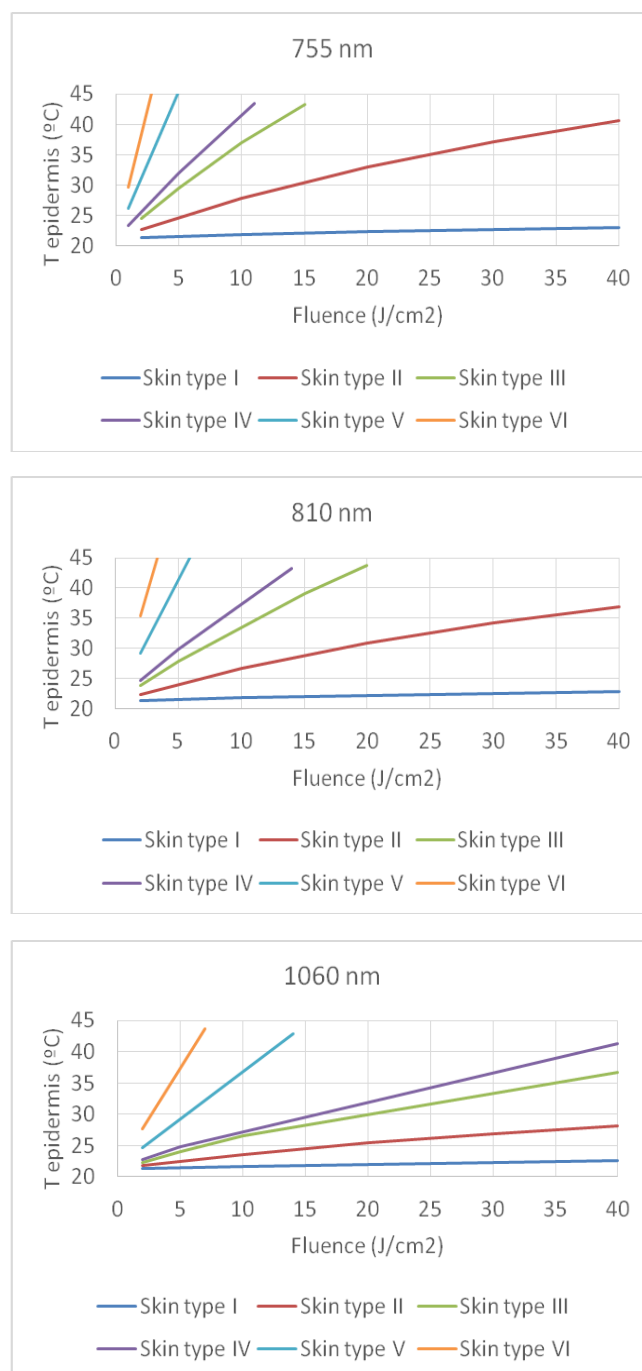


Figure 4: Summarized results of multiple simulations of epidermis temperature with different skin type and laser fluences.

3.2. Evaluation of thermal damage caused by laser using the in silico 3D mathematical model.

We consider the hair removal process to be effective and safe if the laser pulses produce thermal damage in the structure of the hair and surrounding cells without damaging the skin.

In the previous section, the simulation of the epidermis when exposed to the laser beam was demonstrated, which implied an absorption process and resultant heating of this first skin layer. The second consequence of this process is a certain loss of power that will reduce the power available to heat the hair.

Once light reaches the dermis, its diffusion is mainly dominated by scattering. In order to evaluate light scattering within the skin, simulations with hair of the same diameter but different depths were compared. As expected, our model revealed that with increased depth, the effect of scattering reduces the power intensity that can reach the hair, and consequently, a lower temperature is obtained in the deeper hair (Fig. 5A).

Likewise, temperature differences were observed when laser pulses of different wavelengths were compared. For given conditions of pulse duration, the 755 nm laser heats the hair shaft to 174°C, while with the 1060 nm laser the temperature of the hair shaft was just 136°C (Fig. 5B).

Another important factor that should be considered during laser hair removal is the color of the hair. As an example, our 3D model calculated the temperature reached by light and dark hair using a 755 nm and 1060 nm laser respectively (Fig. 5C). For dark hair, the difference in hair temperature when using 755 nm compared to 1060 nm is very large. However, for light hair that contains low levels of melanin, the difference between these two wavelengths is vastly reduced.

Several simulations using the in silico model were performed to compare the results when applying the maximum fluences that do not cause an epidermal temperature of over 43°C with the 755 nm, 810 nm and 1060 nm wavelengths. Table 4 shows an example with the same laser power of 4,000 W, a spot size of 20 x 9 mm², a frequency of 3 Hz, with skin types II and IV and different hair colors and textures. Red, yellow and green are used to highlight conditions without any thermal damage ($\theta_d = 0$), intermediate thermal damage ($0 < \theta_d < 0.63$) and total thermal damage ($0 > 0.63$). Average hair damage is shown, determined from the thermal damage to the hair shaft, bulb, stem cells and growing cells.

For skin type II, a maximum fluence of 40 J/cm² has been considered for the three wavelengths. The simulation results for the epidermis were: 41°C for the 755 nm diode laser, 37°C for the 810 nm diode laser and 28°C for the 1060 nm diode laser. The results for the hair depended on its color and type. For example, for the fine brown hair, the shaft and bulb heated to 172°C and 109°C respectively at 760 nm, 167°C and 110°C at 810 nm and 132°C and 96°C at 1060 nm.

Results show that the heating of the hair is very similar with 755 nm and 810 nm, but substantially higher with 1060 nm. Efficacy can be evaluated from the average hair damage. For fine brown hair, average hair damage was 0.80 for 755 nm, 0.83 for 810 nm and 0.72 for 1060 nm, thus showing that

the three wavelengths can produce total thermal damage of the hair. The same efficacy results were obtained for black hair. For fine light hair, average hair damage was 0.52 for both 755 nm and 810 nm and 0.43 for 1060 nm, thus showing that 755 nm and 810 nm have the same level of efficacy for light hair and are slightly more effective than 1060 nm.

For skin type IV, the maximum fluences that will not cause an epidermal temperature in excess of 43°C, are: 10 J/cm² for a 755 nm diode laser, 14 J/cm² for an 810 nm diode laser and 40 J/cm² for a 1060 nm diode laser. For fine brown hair, the average hair damage was 0.34 for 755 nm, 0.48 for 810 nm and 0.71 for 1060 nm. The same results were obtained for all cases of skin type IV.

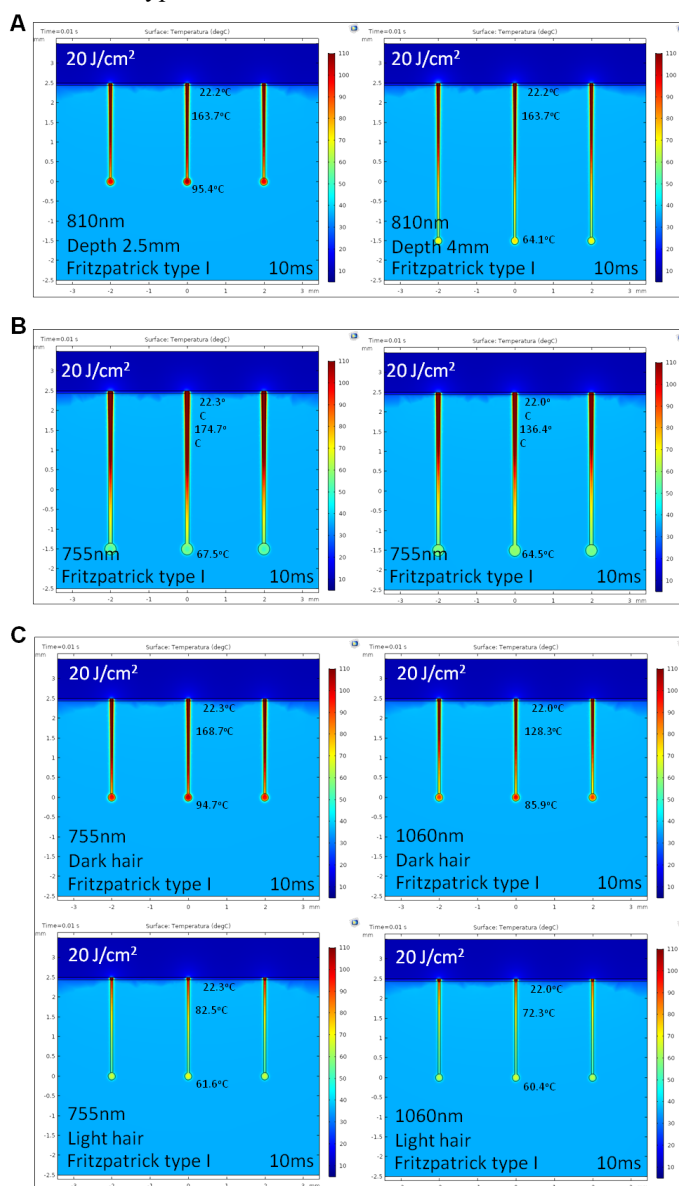


Figure 5: Illustrative examples of simulation results. Simulation of heating of hair with the same dimensions but different depths (A), simulation of laser pulses of different wavelengths (B), an example of temperatures reached by light and dark hair using a 755 nm and 1060 nm laser respectively (C).

TABLE 4: Summary of comparative simulation results for 755 nm, 810 nm and 1060 nm diode lasers, using the same laser power (4,000 W), a spot of 20 x 9 mm², 3 Hz, skin types II and IV and different hair colors and textures.

λ (nm)	Skin type	Hair color	Hair Type	F (J/cm2)	t on (ms)	Epid.		Shaft		Bulbe		Average hair damage			
						T(°C)	θ	T(°C)	θ	T(°C)	θ				
760	II	Light	Fine	40	18	41	94	1.00	56	0.23	72	0.85	48	0.00	0.52
760	II	Light	Thick	40	18	41	102	1.00	55	0.18	57	0.00	40	0.00	0.29
760	II	Brown	Fine	40	18	41	172	1.00	88	0.65	109	1.00	69	0.55	0.80
760	II	Brown	Thick	40	18	41	190	1.00	85	0.70	77	1.00	47	0.00	0.68
760	II	Black	Fine	40	18	41	202	1.00	104	0.75	119	1.00	78	1.00	0.94
760	II	Black	Thick	40	18	41	224	1.00	100	0.80	83	1.00	50	0.00	0.70
810	II	Light	Fine	40	18	37	92	0.95	56	0.23	73	0.90	49	0.00	0.52
810	II	Light	Thick	40	18	37	100	1.00	55	0.20	57	0.05	41	0.00	0.31
810	II	Brown	Fine	40	18	37	167	1.00	86	0.65	110	1.00	69	0.65	0.83
810	II	Brown	Thick	40	18	37	185	1.00	84	0.68	79	1.00	48	0.00	0.67
810	II	Black	Fine	40	18	37	196	1.00	101	0.75	120	1.00	78	1.00	0.94
810	II	Black	Thick	40	18	37	219	1.00	98	0.78	84	1.00	51	0.00	0.69
1060	II	Light	Fine	40	18	28	82	0.80	56	0.23	69	0.70	52	0.00	0.43
1060	II	Light	Thick	40	18	28	90	0.95	56	0.23	56	0.00	42	0.00	0.29
1060	II	Brown	Fine	40	18	28	132	1.00	73	0.53	96	1.00	66	0.35	0.72
1060	II	Brown	Thick	40	18	28	149	1.00	73	0.55	72	0.85	48	0.00	0.60
1060	II	Black	Fine	40	18	28	153	1.00	81	0.60	104	1.00	72	0.80	0.85
1060	II	Black	Thick	40	18	28	174	1.00	81	0.68	77	1.00	50	0.00	0.67
760	IV	Light	Fine	10	5	42	64	0.45	42	0.00	48	0.00	39	0.00	0.11
760	IV	Light	Thick	10	5	42	63	0.45	41	0.00	42	0.00	37	0.00	0.11
760	IV	Brown	Fine	10	5	42	102	1.00	52	0.15	59	0.20	45	0.00	0.34
760	IV	Brown	Thick	10	5	42	100	1.00	49	0.08	48	0.00	39	0.00	0.27
760	IV	Black	Fine	10	5	42	116	1.00	57	0.28	63	0.40	47	0.00	0.42
760	IV	Black	Thick	10	5	42	114	1.00	53	0.18	50	0.00	40	0.00	0.29
810	IV	Light	Fine	14	6	43	70	0.60	44	0.00	52	0.00	41	0.00	0.15
810	IV	Light	Thick	14	6	43	70	0.60	43	0.00	44	0.00	38	0.00	0.15
810	IV	Brown	Fine	14	6	43	115	1.00	57	0.28	68	0.65	48	0.00	0.48
810	IV	Brown	Thick	14	6	43	116	1.00	54	0.20	53	0.00	40	0.00	0.30
810	IV	Black	Fine	14	6	43	133	1.00	63	0.38	72	0.85	52	0.00	0.56
810	IV	Black	Thick	14	6	43	134	1.00	60	0.30	55	0.00	41	0.00	0.33
1060	IV	Light	Fine	40	18	41	81	0.80	56	0.23	69	0.70	52	0.00	0.43
1060	IV	Light	Thick	40	18	41	89	0.95	56	0.23	56	0.00	42	0.00	0.29
1060	IV	Brown	Fine	40	18	41	131	1.00	72	0.50	95	1.00	66	0.35	0.71
1060	IV	Brown	Thick	40	18	41	148	1.00	73	0.55	72	0.85	48	0.00	0.60
1060	IV	Black	Fine	40	18	41	151	1.00	80	0.60	103	1.00	71	0.75	0.84
1060	IV	Black	Thick	40	18	41	172	1.00	81	0.65	76	1.00	50	0.00	0.66

3.3. Determination of the thermal relaxation time (TRT) of the epidermis and hair during laser hair removal

The heating of the hair during laser hair removal depends on pulse duration since the hair is cooled by the surrounding tissue. The hair's own cooling process is known as thermal relaxation time (TRT). It is important to take the TRT of the hair into account when determining the optimal pulse times for hair removal. Interestingly, if the pulse time is less than the thermal relaxation time, effective hair heating is obtained without dermal heating, as can be demonstrated by our 3D model. With longer pulse times, hair is heated less and produces more warming of the dermis, which could induce a higher sensation of pain. As an example, figure 6 shows that a 5 ms laser pulse heated the hair shaft and bulb to 97.1°C and 65.7°C respectively, while a 50 ms laser pulse of the same fluence and wavelength, heated the hair to just 52.2°C and 51.1°C (Fig. 6).

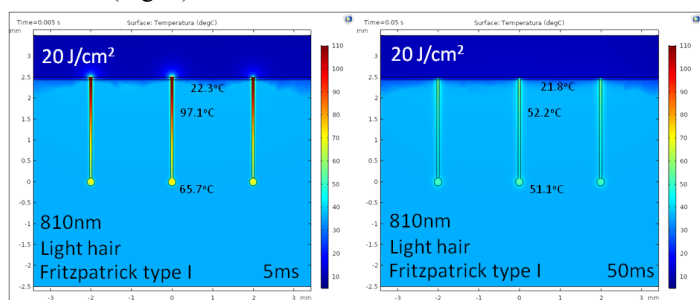


Figure 6: Illustrative example of the thermal relaxation time (TRT) after 5 ms and 50 ms laser pulses respectively.

Based on a series of simulations, we determined the TRT of the epidermis and the hair and its determining factors. TRT is defined as the time required for the temperature to decrease by 50% [24].

The simulation results for the epidermis showed that the TRT of the epidermis is constant with fluence, wavelength, skin type, cooling temperature and spot size. In contrast, the TRT of the epidermis increases linearly with the thickness of the epidermis and depends on the type of cooling. For contact cooling with sapphire windows and a typical thickness of 60 μm, the TRT is 10 ms. However, it has been shown that TRT increases if a layer of gel is added between the skin and the sapphire window. With a gel thickness of 0.3 mm, the TRT is found to increase to 20 ms. On the other hand, if the skin is subject to air cooling instead of contact cooling, it has been calculated that the TRT is 70 ms. A summary of the results is shown in table 5.

TABLE 5: Thermal relaxation time (TRT)

Summary for a typical epidermis 60μm-thick	TRT (ms)
Skin with sapphire contact cooling	10
Skin with sapphire contact cooling plus 0,3mm of gel	20
Skin with air cooling	70

The simulation results for the hair showed that the TRT of the hair is constant with the fluence, wavelength, color and depth. However, the TRT increases linearly with the diameter of the shaft and bulb. The following table 6 shows the TRT results obtained for the different hair diameters.

TABLE 6: Summary of the Thermal Relaxation Times (TRT) obtained for the different hair sizes.

Hair Size	Shaft TRT (ms)	Bulb TRT (ms)
Fine	9	23
Residual fine hair	4	7
Thick	15	50
Residual thick hair	9	23

Residual hair can only be heated efficiently if pulses below 10 ms are used. This demonstrates that to epilate residual hair it is necessary to use very short pulses, and this is only achieved with very high laser power.

Fine hair has a TRT of approximately 20 ms, and thick hair has a TRT of about 50 ms.

Table 7 compares a diode laser of 4,000 W with another of 1,000 W, with the same wavelength of 810 nm, a spot of 20 x 9 mm² and a frequency of 3 Hz. Results for skin types II and IV and for all hair colors and textures are shown. For skin type II, 40 J/cm² is used for both lasers. For example, with the fine brown hair, the shaft and bulb heated to 167°C and 110°C respectively at 4,000 W, and 89°C and 75°C at 1,000 W, which results in average hair damage of 0.83 and 0.56 respectively.

The TRT of fine hair is 9 ms and 23 ms for the shaft and bulb respectively (table 6). The pulse duration for the 4,000 W diode laser at 40 J/cm² is 18 ms, which is similar to the TRT of the fine hair. However, for the 1,000 W diode laser, the pulse duration is 72 nm, which is much longer than the TRT of the fine hair, thus explaining the lower efficacy of this diode laser when compared to the 4,000 W version. The comparison presented in table 6 shows that the hair temperature and thermal damage produced by the 4,000 W laser is substantially higher than with the 1,000 W variant, as explained by the fact that the pulse duration used by the 1,000 W laser is higher than the TRT of the hair, especially for fine hair.

TABLE 7: Summary of simulation results for diode lasers of 4,000 W and 1,000 W, using the same wavelength of 810 nm, a spot of 20 x 9 mm², a frequency of 3 Hz, skin types II and IV and different hair colors and textures.

Power (W)	Skin type	Hair color	Hair Type	Fluence (J/cm ²)	Pulse duration (ms)	Epid. T(°C)	Shaft		Bulbe		Average hair damage				
							Hair T(°C)	Stem cells T(°C)	Hair T(°C)	Growing cells T(°C)					
4000	II	Light	Fine	40	18	37	92	0.95	56	0.23	73	0.90	49	0.00	0.52
4000	II	Light	Thick	40	18	37	100	1.00	55	0.20	57	0.05	41	0.00	0.31
4000	II	Brown	Fine	40	18	37	167	1.00	86	0.65	110	1.00	69	0.65	0.83
4000	II	Brown	Thick	40	18	37	185	1.00	84	0.68	79	1.00	48	0.00	0.67
4000	II	Black	Fine	40	18	37	196	1.00	101	0.75	120	1.00	78	1.00	0.94
4000	II	Black	Thick	40	18	37	219	1.00	98	0.78	84	1.00	51	0.00	0.69
1000	II	Light	Fine	40	72	31	59	0.30	47	0.00	56	0.00	45	0.00	0.08
1000	II	Light	Thick	40	72	31	65	0.45	48	0.00	50	0.00	40	0.00	0.11
1000	II	Brown	Fine	40	72	31	89	0.90	64	0.40	75	0.95	58	0.00	0.56
1000	II	Brown	Thick	40	72	31	102	1.00	66	0.45	64	0.45	45	0.00	0.48
1000	II	Black	Fine	40	72	31	100	1.00	72	0.60	81	1.00	64	0.20	0.70
1000	II	Black	Thick	40	72	31	117	1.00	75	0.65	68	0.65	47	0.00	0.58
4000	IV	Light	Fine	14	6	43	70	0.60	44	0.00	52	0.00	41	0.00	0.15
4000	IV	Light	Thick	14	6	43	70	0.60	43	0.00	44	0.00	38	0.00	0.15
4000	IV	Brown	Fine	14	6	43	115	1.00	57	0.28	68	0.65	48	0.00	0.48
4000	IV	Brown	Thick	14	6	43	116	1.00	54	0.20	53	0.00	40	0.00	0.30
4000	IV	Black	Fine	14	6	43	133	1.00	63	0.38	72	0.85	52	0.00	0.56
4000	IV	Black	Thick	14	6	43	134	1.00	60	0.30	55	0.00	41	0.00	0.33
1000	IV	Light	Fine	25	45	43	55	0.15	44	0.00	52	0.00	43	0.00	0.04
1000	IV	Light	Thick	25	45	43	60	0.35	45	0.00	46	0.00	38	0.00	0.09
1000	IV	Brown	Fine	25	45	43	80	0.80	57	0.23	68	0.65	52	0.00	0.42
1000	IV	Brown	Thick	25	45	43	91	0.95	58	0.23	57	0.00	42	0.00	0.29
1000	IV	Black	Fine	25	45	43	90	0.95	63	0.38	72	0.85	57	0.00	0.54
1000	IV	Black	Thick	25	45	43	103	1.00	65	0.40	59	0.20	44	0.00	0.40

IV. DISCUSSION

This work is intended to enhance comprehension regarding the permanent removal of hair by means of laser irradiation. In order to achieve this goal, a 3D model of hair and skin is proposed in such a manner that both the laser parameters and the biological system properties can be varied and the influence of such variation on the achieved temperature can be analyzed.

We used the COMSOL Multiphysics® mesh to simulate laser hair removal. The COMSOL Multiphysics® program solves the equations numerically for each of the mesh pieces and assembles the results to ultimately provide the solutions of the equations in the whole extent of the domains. The finer the mesh, the more accurate the solution is in the different domains. The problem with a very fine mesh is that the computing time is significantly lengthened, since there will be many elements to calculate. It is necessary to establish a balance between the number of elements and the accuracy of the mesh. The important factors are: i) the number of elements, ii) the minimum element quality and iii) the average element quality. With the data obtained from the numerical simulations it has been possible to obtain a mathematical model that, from the input parameters of the laser shot and the

initial skin and hair conditions, reliably reproduces the temperatures reached by the different hair zones and the skin.

Multiple simulations have been carried out considering all the parameters subject to variation. First, we calculated the epidermal temperature that will be reached for different skin types and laser conditions in order to use our 3D model to guarantee the safety of a patient. Skin type (classified from I to VI according to the Fitzpatrick Classification System) is a key factor to consider when choosing treatment parameters for laser hair removal. The epidermis is the outer layer of skin that contains melanin and is consequently heated by laser absorption. The absorption coefficients of the proteins of melanin (eumelanin and pheomelanin) have been considered in order to correctly simulate the laser interaction with the epidermis of different skin types. The starting temperature of the epidermis (T₀) is determined by the initial cooling conditions: a) sapphire cooling temperature, b) the laser shot frequency which determines the contact time with the cooled sapphire tip before the laser shot is performed, and c) the thickness of the gel layer that is placed between the sapphire and the skin. The increase in temperature depends on four variables: fluence, wavelength, pulse duration and the absorption coefficient determined from the skin type, in addition to other factors—which in this case are only the shape of the spot and the thickness of the epidermis—that have been fixed for this study.

Our model confirms that the heat absorption of the epidermis is due to the presence of eumelanin and increases as the classification number of the skin type increases. As a consequence, skins with a higher skin type classification reach higher temperatures. Notably, the amount of radiation that passes through the epidermis is reduced, thereby reducing the temperature that reaches the hair. The model also confirms that the amount of energy absorbed depends on the wavelength used. Therefore, for high wavelengths, the heating of the epidermis is reduced.

As a main result, the simulation allows the determination of the maximum operation conditions for each wavelength and skin type. Shorter wavelengths have difficulties providing epidermal protection for darker skin due to the higher absorption by melanin. Longer wavelengths have a lower melanin absorption and thus allow using higher fluences.

The scattering coefficient has been considered when simulating the interaction of the laser with the dermis. Water and blood absorption have also been considered, but their effect has been found to produce differences below 10% in the simulation results. Scattering is a process that reduces the amount of laser energy that can reach the hair. Light penetrating the dermis is scattered multiple times before being absorbed by the hair and this is found to increase inversely to the laser wavelength. According to Svaasand & Stuart Nelson, a 755 nm laser is scattered 7.28% more than an 810 nm laser, and 40.4% more than a 1060 nm laser [17]. Therefore, the dependence of the scattering on the wavelength has been found to be the main factor affecting the laser-dermis interaction considered in our model.

Furthermore, we have calculated thermal damage caused by laser hair removal. Hair comprising a cylindrical shaft with

specific dimensions (length and diameter), a spherical bulb and two sheaths containing cells, has been designed in our model. To achieve definitive hair removal, the tissue containing the stem cells (located in the bulge) must be damaged as well. For this, it is necessary to further increase the temperature of the hair so that it reaches and destroys the stem cells via thermal conduction. The model clearly shows that the higher the fluence, the greater the thermal damage caused to the hair structure. But it also shows that fluence alone does not determine how the energy will be absorbed by the target tissue. The wavelength of the energy and characteristics of the hair (color and texture) are also key factors of thermal damage.

Finally, based on our 3D model, we can also calculate the TRT of the tissues. TRT is essential for understanding the laser technology of short pulse hair removal. It allows us to know the optimal pulse time for hair removal without damaging the skin. Therefore, its significance and definition are very important in order to guarantee the effective and painless removal of the hair of every patient. Firstly, we have demonstrated that the type of cooling changes the TRT of the skin. Contact cooling using a cold sapphire crystal provides more efficient protection than gel or air cooling because it provides faster removal of the heat generated in the epidermis during the laser pulse. Secondly, the TRT of the hair depends on its diameter, since this determines its surface area to volume ratio. Hairs with smaller diameters have a high surface to volume ratio, so they cool much more quickly than thicker hairs. Differences in TRT are a key factor in laser hair removal. Thirdly, pulse duration is the key parameter for maximizing the effectiveness of hair removal. High power allows shorter pulse durations, which enhances the heating of the hair due to TRT. Laser pulses shorter than the TRT result in efficient heating of the hair follicle and surrounding structures. Pulses longer than the TRT may result in insufficient heating of the target.

V. CONCLUSIONS

Numerical simulation using light diffusion, heat transfer and thermal damage 3D equations has been used to simulate the process of laser hair removal. Diode lasers of 4,000 W and 1,000 W, with wavelengths of 755 nm, 810 nm and 1060 nm, and spot sizes of 20 x 9 mm² have been simulated.

Consequently, pulses of light which are shorter than the thermal relaxation time of the hair (4–50 ms) have been shown to efficiently heat and damage the hair follicle. The higher the fluence, the greater the damage to the hair structure will be. However, the fluence is limited by the absorption of the epidermis which is dependent on the skin type and the laser wavelength. For low numbered skin types (I and II), high fluence can be used for all wavelengths, from 755 nm to 1060 nm. However, for high numbered skin types, the maximum fluence for each wavelength is limited by the epidermal absorption, especially for the 755 nm wavelength. Best results are obtained with 1060 nm laser diodes since they allow the use of a higher fluence without damaging the skin.

In summary, we have demonstrated that the simulation can be used to predict the thermal injury to the hair follicle without

damaging the skin with the proper epidermis cooling, pulse energy, pulse duration and wavelength.

ACKNOWLEDGMENT

We would like to acknowledge Petra Gener for general administrative support, writing assistance and/or technical editing, language editing, and proofreading. A special mention to Pablo Garcia for his valuable contribution to this research.

REFERENCES

- [1] Grossman MC, Dierickx, C, Farinelli W, et al. "Damage to hair follicles by normal-mode ruby laser pulses." *J Am Acad Dermatol* 35:889, 1996.;
- [2] Lars O. Svaasand, J. Stuart Nelson; "On the physics of laser-induced selective photothermolysis of hair follicles: Influence of wavelength, pulse duration, and epidermal cooling.", *Journal of Biomedical Optics* 9(2), 353–361 (March/April 2004);
- [3] M. A. Trelles; Francisco Camacho Martínez; J.L. Cisneros, "Láser en dermatología y dermocosmética.", Ed. Aula Médica, Spain, 2008.
- [4] Barbara Buffoli, PhD, Fabio Rinaldi, MD, Mauro Labanca, MD, Elisabetta Sorbellini, MD, Anna Trink, MD, Elena Guanziroli, MD, Rita Rezzani, PhD, and Luigi F. Rodella, MD, "The human hair: from anatomy to physiology.", *International Journal of Dermatology* 2014, 53, 331–341;
- [5] Robert M. Lavker, Tung-Tien Sun, Hideo Oshima, Yann Barrandon, Masashi Akiyama, Corinne Ferraris, Genevieve Chevalier, Bertrand Favier, Colin A. B. Jahoda, Danielle Dhouailly, Andrei A. Panteleyev, and Angela M. Christiano, "Hair Follicle Stem Cells.", *JID Symposium Proceedings*, Vol. 8, No. 1 June 2003.
- [6] K. Robertson, J. L. Rees. "Variation in Epidermal Morphology in Human Skin at Different Body Sites as Measured by Reflectance Confocal Microscopy". *Acta Derm Venereol* 90, 368-373, 2010.
- [7] L. Cheung, D. Mitrea, C. Suhlrand, H. Zeng. "Laser Hair Removal: Comparative Study of Light Wavelength and its Effect on Laser Hair Removal". BEE 4530 Final Project, 2009.
- [8] G. Lask, M. Elman, M. Slatkine, A. Waldman, Z. Rozenberg. "Laser-assisted Hair Removal by Selective Photothermolysis". *American Society for Dermatologic Surgery* 23, 737-739, 1997.
- [9] G.B. Altshuler, R.R. Anderson, D. Manstein, H.H. Zenzie, M.Z. Smirnov. "Extended Theory of Selective Photothermolysis". *Lasers in Surgery and Medicine* 29, 416-432, 2001].
- [10] C. Donner, H.W. Jensen. "A Spectral BSSRDF for Shading Human Skin". *Eurographics Symposium on Rendering*, 2006.
- [11] S.L. Jacques. "Skin Optics". *Oregon Medical Laser Center News*, 1998).
- [12] T. van Kampen. "Optical properties of hair". Thesis from Technical University Eindhoven, 1997.
- [13] Linhong Kou, Daniel Labrie, and Petr Chylek. "Refractive indices of water and ice in the 0.65- to 2.5- μ m spectral range" *Optical Society of America*, 1993.
- [14] S. Takatani and M. D. Graham, "Theoretical analysis of diffuse reflectance from a two-layer tissue model," *IEEE Trans. Biomed. Eng.*, BME-26, 656--664, (1987).
- [15] Laura A. Sordillo, Yang Pu, Sebastiao Pratavieira, Yury Budansky and Robert R. Alfano, "Deep optical imaging of tissue using the second and third near infrared spectral windows", *Journal of Biomedical Optics* 19(5), 2014".
- [16] W. Verkruysse, R. Zhang, B. Choi, G. Lucassen, L. O. Svaasand, J. S. Nelson. "A library based fitting method for visual reflectance spectroscopy of human skin". *Physics in Medicine and Biology* 50, 57-70, 2005.
- [17] L.O. Svaasand, J.S. Nelson. "On the physics of laser-induced selective photothermolysis of hair follicles: Influence of wavelength, pulse duration, and epidermal cooling". *Journal of Biomedical Optics* 9(2), 353–361 2004)
- [18] C. Ash, K. Donne, G. Daniel, G. Town, M. Clement, R. Valentine. "Mathematical modeling of the optimum pulse structure for safe and effective photo epilation using broadband pulsed light". *Journal of Applied Clinical Medical Physics* Vol. 13, No 5, 2012.
- [19] L. Cheung, D. Mitrea, C. Suhlrand, H. Zeng. "Laser Hair Removal: Comparative Study of Light Wavelength and its Effect on Laser Hair Removal". BEE 4530 Final Project, 2009.



- [20] T. J. Pfefer, J. K. Barton, D. J. Smithies, T. E. Milner, J. S. Nelson, M. J. C. van Gemert, A J. Welch. "Modeling Laser Treatment of Port Wine Stains with a Computer-Reconstructed Biopsy". *Lasers in Surgery and Medicine* 24, 151-166, 1999.
- [21] <http://www.guilloptics.com/sapphire-properties/sapphire-properties/>
- [22] <http://www.matweb.com>
- [23] F. Xu • T. J. Lu • K. A. Seffen. "Biothermomechanical behavior of skin tissue", *Acta Mech Sin* (2008) 24:1–23.
- [24] M. J. Murphy & P. A. Torstensson. "Thermal relaxation times: an outdated concept in photothermal treatments". *Lasers Med Sci* 29:973–978, 2014.
- [25] C Sturesson and S Andersson-Engels, "Mathematical modelling of dynamic cooling and pre-heating, used to increase the depth of selective damage to blood vessels in laser treatment of port wine stains.", Division of Atomic Physics, Lund Institute of Technology, PO Box 118, S-221 00 Lund, Sweden, *Phys. Med. Biol.* 41 (1996) 413–428.